

Modulation response of VCSELs: a physics-based simulation approach

Original

Modulation response of VCSELs: a physics-based simulation approach / Gullino, Alberto; Tibaldi, Alberto; Bertazzi, Francesco; Goano, Michele; Daubenschuz, Markus; Michalzik, Rainer; Debernardi, Pierluigi. - STAMPA. - (2020), pp. 65-66. (Intervento presentato al convegno 20th International Conference on Numerical Simulation of Optoelectronic Devices (NUSOD 2020) tenutosi a Online conference nel September 2020) [10.1109/NUSOD49422.2020.9217650].

Availability:

This version is available at: 11583/2848156 since: 2020-10-12T16:34:23Z

Publisher:

IEEE

Published

DOI:10.1109/NUSOD49422.2020.9217650

Terms of use:

This article is made available under terms and conditions as specified in the corresponding bibliographic description in the repository

Publisher copyright

IEEE postprint/Author's Accepted Manuscript

©2020 IEEE. Personal use of this material is permitted. Permission from IEEE must be obtained for all other uses, in any current or future media, including reprinting/republishing this material for advertising or promotional purposes, creating new collecting works, for resale or lists, or reuse of any copyrighted component of this work in other works.

(Article begins on next page)

Modulation response of VCSELs: a physics-based simulation approach

Alberto Gullino*, Alberto Tibaldi*[†], Francesco Bertazzi*[†], Michele Goano*[†], Markus Daubenschütz[‡],
Rainer Michalzik[§] and Pierluigi Debernardi[†]

* Dipartimento di Elettronica e Telecomunicazioni, Politecnico di Torino, Corso Duca degli Abruzzi 24, 10129 Torino, Italy

[†] CNR-IEIIT, Corso Duca degli Abruzzi 24, 10129 Torino, Italy

[‡] TRUMPF Photonic Components GmbH, 89081 Ulm, Germany

[§] Institute of Functional Nanosystems, Ulm University, 89081 Ulm, Germany

E-mail: alberto.gullino@polito.it

Abstract—A preliminary study of the dynamic behaviour of a GaAs/AlGaAs 850 nm VCSEL is presented, with the focus on the small-signal analysis and in particular on the optical amplitude modulation response. Simulations are performed with our in-house quantum-corrected one-dimensional drift-diffusion code D1ANA, updated to perform the AC analysis. The -3 dB cutoff frequency of the device is extracted as a function of VCSEL bias current and compared with experimental results.

I. INTRODUCTION

The paradigm dominating the ICT scene is centralized computation, where the majority of data traffic is localized in huge data centres [1]. Therefore, short-range interconnects are assuming a role comparable or even greater as that of telecommunications, as the market is requiring maximum modulation speed with minimum power consumption [2]-[5]. In this context, 850-980 nm vertical-cavity surface-emitting lasers (VCSELs) appear as key technology enablers for intra-datacentre links within 1 km. Still, the present time to market is not compatible with the long and expensive prototyping steps, so that computer-aided design (CAD) appears as the only viable instrument to trace the roadmap for the next generation of high-speed VCSELs. In this view, our research group developed the in-house three-dimensional solver VENUS [6], able to simulate in a self-consistent fashion the electrical, optical and thermal problems at steady state.

This work is our preliminary step to upgrade VENUS with small-signal modulation features. This is investigated on our in-house 1D drift-diffusion code D1ANA (drift-diffusion 1D-ANALysis). Even though less realistic than VENUS, D1ANA is about 100 times faster than it. In this view, D1ANA could be thought as an intermediate model between fully-phenomenological rate equations and entirely-physics-based 3D pictures, efficient enough to be applied to extended parametric campaigns and/or in optimization loops. The simulation framework is validated first with Synopsys Sentaurus Device (electrical-only characteristics), and then with experimental results.

II. RESULTS AND OUTLOOKS

The investigated device is the oxide-confined AlGaAs VCSEL reported in [7, fig. 1]. This features a 1λ -cavity embedding three 8 nm GaAs quantum wells (QWs). The cavity,

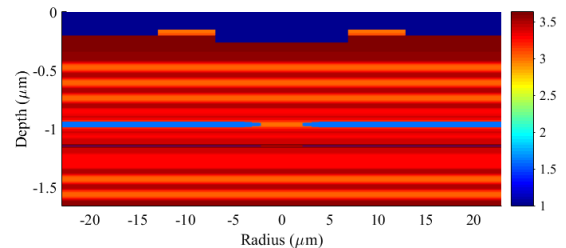


Fig. 1: Refractive index transverse section of the optical structure in a compact form (DBR multiplicity skipped) of investigated VCSEL [7]. Blue region ($n = 1$) indicates air; the two relieves at the top are the metal contact placed above the a p^{++} -doped GaAs layer; the region between two light blue stripes is the oxide aperture. Below the QW region. The 110nm thick substrate is not shown.

lasing at $\lambda = 850$ nm, is defined by a bottom n -doped and a top p -doped distributed Bragg reflectors (DBRs), both composition- and doping-graded to improve carrier transport and free-carrier absorption losses. The 30 nm thick oxide layer has an aperture of diameter $4.7 \mu\text{m}$, which provides both current and optical confinements. This structure lies on a $110 \mu\text{m}$ thick n -type GaAs substrate. The top metallic contact is made of a metal ring (radius $6 \mu\text{m}$) deposited on the topmost GaAs layer, where an ohmic contact is realized with a heavy p^{++} doping.

D1ANA is applied to a vertical cut taken at the axis center of the axisymmetric structure depicted in Fig. 1. The DBRs are described including all the doping and compositional details only in the proximity of the active region (4 pairs at each side), while an electrically-equivalent medium is adopted elsewhere [8], [9], [10]. The vertical cut steps through the oxide aperture, assuming the position of the top contact as aligned to the aperture, therefore not including every lateral transport effect.

D1ANA is based on the drift-diffusion model [11], thus it solves in a self-consistent fashion the Poisson's equation with the carrier continuity equations. Fermi-Dirac statistics [12], [13] is used to describe electron and hole densities, together with the incomplete ionization model of the dopants. *Quantum corrections* are taken into account to model properly the active region containing QWs [14]. This is accomplished by introducing 2D and 3D active region carrier populations

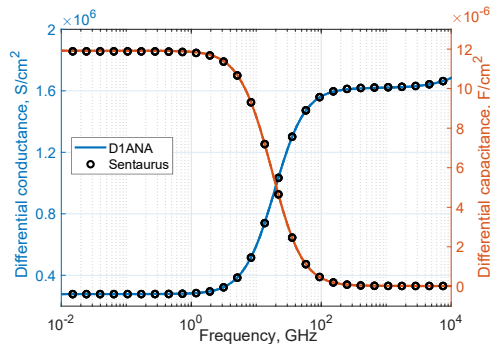


Fig. 2: Comparison of differential conductance and capacitance spectra of a *pin* diode (300 nm *p*-type 10^{19} cm^{-3} doped; 10 nm intrinsic layer; 300 nm *n*-type 10^{19} cm^{-3} doped), computed by D1ANA and Sentaurus Device.

and coupling them through a capture time. Optical data, such as modal losses, optical confinement factor and output power coupling coefficient, are extracted from our in-house solver VELM [15], [16], and plugged in D1ANA to describe coupling between carriers and photons. The gain model is based on Fermi's golden rule and electronic band structure is computed by means of Köhl-Luttinger Hamiltonian approach.

The AC analysis is performed at every steady-state point above threshold, starting from the system Jacobian. This is already available as the major ingredient for the solution of the non-linear drift-diffusion system through the Newton's method. Therefore, at convergence the AC analysis is readily available. Our solver is validated by comparing the small-signal features of simple *pin* structure with a commercial simulator, as shown Fig. 2. It is to be remarked that this validation is pertinent only to the electrical features, since, to the best of our knowledge, no commercial simulator implements both the AC analysis and quantum corrections/photon rate equations.

Then, the 1D code is applied to reproduce the experimental DC characteristics. The key point to connect the 1D to 3D worlds is the effective area. This is computed starting from oxide aperture ($4.7 \mu\text{m}$ diameter) and including a fitting "size factor", which accounts for the actual 3D features, such as annular contact ring and lateral diffusion. A size factor of 1.7 provides a very good match between experimental and computed data (see inset in Fig. 3). At present, no thermal effect is included in D1ANA; the features of a purely 1D heat transport will be investigated later. For this reason, it is meaningful to test the model only in the linear part of the *LI* characteristic, which is the case for $I = 1$ and 2 mA. In order to include the effect of parasitics, an external RC parasitic network is introduced. A best fit is achieved by placing a pole at 2 GHz. The computed amplitude (normalized) modulation response of the device is shown in Fig. 3 as continuous lines, together with the experimental curves (circles), which display the well know oscillation relaxation peak. As the current increases, the optical response of the VCSEL has a flatter peak shifted at higher frequency, and features higher speed. In fact, photon and carrier modulation follows current modulation for frequencies up to relaxation, which in turn depends on

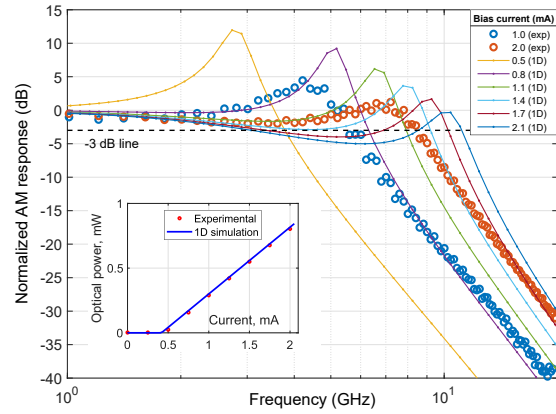


Fig. 3: Normalized amplitude modulation vs frequency plot for various bias currents. Open circles refer to experimental data at 1 and 2 mA; solid lines to model results. The inset shows the experimental (red circles) and D1ANA (solid blue line) *LI* curve up to 2 mA.

the bias current itself, and then drops. This is shown in the computed spectra superimposed to the experiments, in a range of currents from 0.5 to 2 mA. Even though the overall behavior is captured, still we do not have a perfect matching at equal current values. We instead observe a nice fit for currents smaller than in the experiments by some 20%. Further work will address this issue, starting from thermal phenomena, which are good candidate for the differences we observe.

REFERENCES

- [1] Y.-C. Chang and L. A. Coldren, "Design and Performance of High-Speed VCSELs", in *VCSELs*, Ed. R. Michalzik, Springer Series in Optical Science 166, ch. 7, pp. 233-262 (2013)
- [2] G. Ghione, *Semiconductor Devices for High-Speed Optoelectronics*, Ed. Cambridge University Press, ch. 5, pp 317-318 (2009)
- [3] H. Moench, *et al.*, in *Proc. SPIE 9766*, 97 660A-1-16 (2016)
- [4]
- [5] R. Michalzik, "VCSEL Fundamentals", in *VCSELs*, Ed. R. Michalzik, Springer Series in Optical Science 166, ch. 2, pp. 19-75 (2013)
- [6] A. Tibaldi, F. Bertazzi, M. Goano, R. Michalzik, P. Debernardi, "VENUS: A Vertical-Cavity Surface-Emitting Laser Electro-Opto-Thermal Numerical Simulator", in *IEEE Journ. of Sel. Topics in Quant. Electronics* **25**, 1500212 (2019)
- [7] A. Tibaldi, F. Bertazzi, M. Goano, R. Michalzik, P. Debernardi, M. Daubenschütz, "Probing Thermal Effects in VCSELs by Experiment-Driven Multiphysics Modeling", in *IEEE J. Select. Topics Quantum Electron.* **25**, 1500212 (2019)
- [8] M. Calciati, A. Tibaldi, F. Bertazzi, M. Goano, P. Debernardi, *Semiconductor Sci. Tech.* **32**, 055007 (2017)
- [9] M. Streiff, *et al.*, in *IEEE Journ. of Sel. Topics in Quant. Electronics* **9**, pp. 879-891 (2003)
- [10] M. Farzaneh, *et al.*, in *IEEE Photon. Technol. Lett.* **19**, pp. 601-603 (2007)
- [11] R. Sacco, *et al.*, in *Journal of Computational Physics* **204**, pp. 533-561 (2005)
- [12] J. S. Blakemore, in *Solid State Electronics* **25**, pp. 1067-1076 (1982)
- [13] M. Goano, in *Solid State Electronics* **36**, pp. 217-221 (1993)
- [14] M. Grupen and K. Hess, in *IEEE Journ. of Quant. Electr.* **34**, pp. 120-140 (1998)
- [15] G. P. Bava, P. Debernardi, and L. Fratta, "Three-dimensional model for vectorial fields in vertical-cavity surface-emitting lasers", in *Phys. Rev. A* **63**, pp. 23816-1-23 816-13 (2001)
- [16] P. Debernardi and G. P. Bava, "Coupled mode theory: a powerful tool for analyzing complex VCSELs and designing advanced devices features", in *IEEE Journ. of Sel. Topics in Quant. Electronics* **9**, pp. 905-917 (2003)